



HAL
open science

Can Multiscale Thermal Infrared Imaging Help Validate and Monitor Water Stress in Alluvial Forests?

Julien Godfroy, Pauline Malherbe, Flavie Gerle, Baptiste Marteau, Pierre Lochin, Sara Puijalon, Jérôme Lejot, Antoine Vernay, Hervé Piégay

► **To cite this version:**

Julien Godfroy, Pauline Malherbe, Flavie Gerle, Baptiste Marteau, Pierre Lochin, et al.. Can Multiscale Thermal Infrared Imaging Help Validate and Monitor Water Stress in Alluvial Forests?. *Ecohydrology*, 2024, 10.1002/eco.2710 . hal-04727497

HAL Id: hal-04727497

<https://hal.science/hal-04727497v1>

Submitted on 9 Oct 2024

HAL is a multi-disciplinary open access archive for the deposit and dissemination of scientific research documents, whether they are published or not. The documents may come from teaching and research institutions in France or abroad, or from public or private research centers.




L'archive ouverte pluridisciplinaire **HAL**, est destinée au dépôt et à la diffusion de documents scientifiques de niveau recherche, publiés ou non, émanant des établissements d'enseignement et de recherche français ou étrangers, des laboratoires publics ou privés.



Distributed under a Creative Commons Attribution - NonCommercial 4.0 International License

RESEARCH ARTICLE OPEN ACCESS

Can Multiscale Thermal Infrared Imaging Help Validate and Monitor Water Stress in Alluvial Forests?

Julien Godfroy^{1,2}  | Pauline Malherbe¹ | Flavie Gerle³ | Baptiste Marteau^{1,4} | Pierre Lochin¹  | Sara Puijalon³ | Jérôme Lejot⁵ | Antoine Vernay³  | Hervé Piégay¹

¹University of Lyon, ENS Lyon, CNRS, UMR 5600 EVS, Lyon, France | ²Université Grenoble Alpes, INRAE, LESSEM, St-Martin d'Hères, France | ³University of Lyon, Université Claude Bernard Lyon 1, LEHNA UMR 5023, CNRS, ENTPE, Villeurbanne, France | ⁴Université Rennes 2, UMR6554 LETG, Rennes, France | ⁵University of Lyon, Université Lumière Lyon 2, CNRS, UMR 5600 EVS, Lyon, France

Correspondence: Julien Godfroy (julien.godfroy@inrae.fr)

Received: 23 April 2024 | **Revised:** 7 August 2024 | **Accepted:** 13 August 2024

Funding: This research was funded with the support of the Graduate School H2O'Lyon (ANR-17-EURE-0018) of the Université of Lyon (UdL), which is part of the programme 'Investissements d'Avenir' operated by Agence Nationale de la Recherche (ANR). This work was also carried out within the framework of the Fédération de Recherche BioEEnViS. The work of Julien Godfroy was also supported by the Agence de l'Eau Rhône Méditerranée Corse. The work of Pierre Lochin was supported by the Graduate School H2O'Lyon and by the US National Science Foundation (EAR 1700517 and EAR 1700555). Baptiste Marteau's contribution was partly funded through the national 'Plan de Relance' programme coordinated by ANR.

Keywords: anthropogenic alterations | drought | multi-method approach | riparian vegetation | thermal infrared remote sensing | water stress

ABSTRACT

Alluvial forests are sensitive to drought induced by climate change and exacerbated by altered flow regimes. Our ability to detect and map their sensitivity to drought is crucial to evaluate the effects of climate change and adjust management practices. Therefore, we explore the potential of multiscale thermal infrared imagery (TIR) to diagnose their sensitivity to droughts. In summer 2022, we sampled leaves and phloem on *Populus nigra* trees from two sites with contrasted hydrological connectivity along the Ain River (France) to investigate the seasonality of water stress and act as ground truth for airborne TIR images. To map forest sensitivity to drought, we used TIR data from four airborne campaigns and Landsat archives over a larger spatial and temporal extent. Field data showed that stress conditions were reached for both sites but were higher in the site with lower groundwater connectivity, which was also the case for individual tree crown temperatures. At the forest plot scale, canopy temperature was linked to forest connectivity for two of four TIR campaigns, with higher values in the more degraded reaches. Landsat data were used to locate the areas of the riparian forest impacted by a historical drought event and monitor their recovery and proved useful to identify trends. TIR data showed promising results to help detect and map tree water stress in riparian environments. However, stress is not detected in all TIR campaigns, demonstrating that one-shot TIR acquisitions alone are not enough to diagnose stress and complementary in-field eco-physiological measurements are necessary.

1 | Introduction

Alluvial forests are unique environments characterized by complex feedback processes with their river system that provide a set of ecosystem services (Naiman et al. 1988; Riis et al. 2020). Alluvial forests are biodiversity hotspots (Naiman, Decamps, and Pollock 1993), improve water quality (Dosskey et al. 2010;

Tabacchi et al. 2000), help stabilize channel banks (Simon and Collison 2002) and play a key role in ensuring the sustainability of good hydromorphological conditions in river systems (González del Tánago et al. 2021).

Human development in the 20th century has however caused increased pressure on riparian vegetation (Bravard

et al. 1997; Breton, Girel, and Janssen 2023; Comiti et al. 2011; Poff et al. 2007). Activities such as gravel mining, damming and engineering works have induced tree stress and increased mortality (Scott, Lines, and Auble 2000) and led to a reduction of forest renewal by increasing bank resistance or reducing channel mobility in other cases (Décamps et al. 1988; Dépret et al. 2023). Key riparian species are also sensitive to climate change (O'Briain 2019). Higher temperatures and variations in precipitations and flow regimes brought about by climate change can impact tree water use and water availability (Rivaes et al. 2013; Stella et al. 2013). Groundwater decline due to drought or anthropogenic alterations can induce stress and higher mortality in riparian woodlands and lead to long-term shifts in species composition (Breton, Girel, and Janssen 2023; Janssen et al. 2020; Kibler et al. 2021; Rohde et al. 2021).

Therefore, it is important to monitor the response of riparian vegetation to events affecting water availability such as channel incision due to damming or mining and droughts due to climate change. Such a monitoring effort can then help target conservation and restoration actions to mitigate negative impacts of global change on riparian forests and assess their efficiency.

Field surveys are traditionally used to assess the water status of individual trees. For example, tree rings can give insights into events happening within the lifespan of an individual and radial growth anomalies can occur during dryer years (Dufour and Piégay 2008; Singer et al. 2013; Stella et al. 2013). Other less destructive methods such as sampling tree leaves or phloem can also inform about tree water status. The measure of leaf water potential (LWP) can indicate ongoing water stress of the tree at the time of sampling (Brodrribb and Holbrook 2003; Scholander et al. 1965). Carbon isotope analysis of the phloem content can help determine how efficient a tree is at using water to produce biomass (intrinsic water use efficiency [iWUE]), which responds to water deficits such as drought-related stress (Klein et al. 2016; Seibt et al. 2008). One of the main limitations of such approaches however is that they are time-intensive and cannot easily be conducted at a large scale within a short time window.

At the scale of communities or river reaches, remote sensing has been used to assess forest status with imagery in the visible and near-infrared (NIR) spectrum (Kibler et al. 2021) or in the thermal infrared (TIR) spectrum (Mayes et al. 2020). In these cases, TIR data are used because differences in canopy temperatures are a good indicator of differences in evapotranspiration. Even though remote sensing applications are increasingly common to study riparian vegetation, the use of TIR sensors has been mostly limited to the use of satellite-based sensors in arid or semi-arid climates where drought events are common today (Table 1).

One of the advantages of using data from satellites is that they can cover large spatial scales at a temporal resolution that cannot be matched by airborne surveys (e.g., 8-day repeat coverage for Landsat data and an 8-day repeat cycle with near-daily coverage of a given zone for MODIS data). This enables monitoring the impact of specific climate events by investigating the consequences of drought or changes in groundwater accessibility on

water use by riparian trees (Lurtz et al. 2020; Mayes et al. 2020). A key disadvantage of satellite data, however, is that spatial resolution is coarse for spectral bands in the TIR region, for instance, with 100 m at-sensor resolution for Landsat 8 and 9, which is then resampled afterwards to fit the 30 m resolution of Landsat products.

Finer spatial resolution is available when mounting TIR sensors on airborne vectors such as an airplane or an unmanned aerial vehicle (UAV) and can also be used to assess the health status of the vegetation or evapotranspiration (Neale et al. 2011). A recent study showed that it was possible to detect genetic trait differences between cottonwood trees from different populations planted in the same plantation (Sankey et al. 2021). This suggests that airborne TIR imagery can also provide critical insights into riparian vegetation, but studies using such vectors are rare.

Additionally, for aircraft acquisitions that can provide the combination of spatial extent and resolution, which is the most interesting to stakeholders, acquiring repeated observations over an entire phenological seasons is usually difficult. Although airborne TIR images are not often used to assess vegetation health, acquisitions over river corridors are already frequent and have led to multiple publications focusing on the surface temperature of rivers (see, for instance, a guide aimed at practitioners; Dugdale 2016). Indeed, knowledge of river temperature helps target areas of ecological interest for species living in the river and helps conservation efforts. Thermal refuges are of increasingly high importance for species in warming waters (Dugdale et al. 2016; Wilbur et al. 2020), and monitoring the thermal functioning of rivers provides insights to assess the impact of restoration projects (Marteau, Michel, and Piégay 2022). Data acquired for such studies also cover riparian vegetation but usually only focuses on the shading effects provided by trees and on their ability to lower water temperature during summer (Dugdale et al. 2018; Marteau et al. 2022; Wawrzyniak et al. 2017; Whitley et al. 2006).

Therefore, TIR data are available from either satellite or airborne sensors with promising potential to provide feedback about riparian vegetation health, but this potential has yet to be assessed and confronted to in-field eco-physiological measurements of water stress in the riparian environment.

In this context, this study aims at exploring the potential of multiscale TIR data to diagnose the sensitivity of riparian forests to drought events.

To address those aims, we (1) tested the validity of TIR information as a good indicator of water stress by coupling field evidence from ecophysiological surveys conducted at an individual scale during summer 2022 with a simultaneous TIR acquisition during the peak of the drought period. This enabled (2) the comparison of four existing historical airborne TIR acquisitions to study the response sensitivity of the forest to a set of potential drought events over a 50 km reach and then (3) the replication of a similar temporal analysis using TIR satellite data in order to identify lasting changes at the corridor scale over a longer time scale (e.g., 34 years).

TABLE 1 | Examples of recent thermal infrared studies focusing on riparian vegetation.

Study	Sensor	Vector	Objective	Climate	Time series
Neale et al. (2011)	FLIR SC640	Aircraft	Estimating evapotranspiration	Mediterranean (California)	
Gokool et al. (2017)	MODIS + Landsat	Satellite	Retrieving daily evapotranspiration from satellite data	Semi-arid (South Africa)	X
Fairfax and Small (2018)	Landsat	Satellite	Assessing the impact of beaver damming on evapotranspiration	Arid (Nevada)	X
Lurtz et al. (2020)	Landsat	Satellite	Relationship between evapotranspiration and modelled water table depths	Semi-arid (Colorado)	X
Ciężkowski, Kleniewska, and Chormański (2020)	Landsat	Satellite	Comparing thermal and optical indexes to detect stress	Temperate transitional (Poland)	X
Mayes et al. (2020)	Landsat	Satellite	Understanding water use at landscape scale	Semi-arid (Mexico)	X
Sankey et al. (2021)	SenseFly ThermoMAP	UAV	Detecting genetic traits differences	Semi-arid (Central Arizona)	

Our chosen study site was the riparian corridor of the Ain River because (1) it is large enough to be approached using Landsat imagery, (2) airborne TIR images have historically been acquired over the corridor to study river temperature and (3) the forest is dominated by the phreatophyte *Populus nigra* populations established on sites with contrasting connectivity to the river.

2 | Study Site

The Ain River is one of the main tributaries of the upper Rhône River in France. During the 20th century, a chain of dams was built on this large, meandering gravel-bed river for hydroelectric purposes, causing a sediment starvation that propagates downstream by 500 m per year on average and results in a channel incision of 1–2 m (Rollet 2007; Rollet et al. 2014). We focus on a 50-km-long reach that starts downstream of this chain of dams and ends at the confluence with the Rhône River, which is referred to as the lower Ain River valley (Figure 1). The upstream section of the lower Ain River (R1) is characterized by sediment starvation and channel incision induced by the upstream dams. Downstream from this incised reach, elevation of the riverbed is stable, and active channel meandering occurs and rejuvenates the riparian forest (R2). Further downstream is another reach affected by sediment starvation because of the combined effects of sediment trapping in R2 and limited local production due to lateral constraints by morainic deposits (R3). Finally, the reach of the river that leads to its confluence with the Rhône River has been historically affected by regressive incision from the Rhône River but now produces enough sediment due to

channel meandering to lead to aggradation near the confluence in recent years (R4).

Traditional on-field forestry surveys conducted in 2008 and 2017 by the French National Forestry Office (ONF) (Dumas 2017; Dumas and Perrin 2006) showed that the dominant species in the riparian forest is *P. nigra*. These studies also suggested that sediment starvation and channel incision have an impact on the health of the riparian forest along the Ain River, with a relative loss of native pioneer species (*P. nigra*, *Salix alba*, *Salix eleagnos*) in favour of exotic (*Fallopia japonica*) or post-pioneer (*Fraxinus excelsior*) species. They also mention high mortality of poplar trees in the sector near the confluence that they attribute to drought events in the early 2000s.

This degraded health status of the riparian forest is visible as a downward trend in NDVI from Landsat images (Lejot et al. 2011) as well as from a study looking at the long-term impacts of channel incision by coupling the data from the ONF field surveys with LiDAR and hyperspectral datasets (Godfroy et al. 2023). This later study highlighted that in reach R1, the relative elevation of the riparian forest from the base flow waterline is higher than in reach R2, which results in an increased distance to the groundwater table and a dryer environment. The Ain River is therefore an interesting site to address our aims because the known changes in forest composition, structure and reflectance in the visible and NIR spectrum based on forest stationary conditions suggest that water stress occurs during the growing period and that some poplar trees are known to have responded to a dryer environment.

3 | Materials and Methods

3.1 | Forestry Data Used for Field Validation

Fieldwork was conducted approximately every 2 weeks between 5 May and 27 September 2022 (Table A1). It focused on two sampling sites with differing geomorphic conditions: a site on the R2 reach where poplar trees were assumed to be well connected to the river system (W+) and a site on the R1 reach where poplars were assumed to be disconnected from the river and to have more limited access to groundwater (W–). Site selection was based on previous work on the riparian forest by Dufour (2005) and Godfroy et al. (2023).

For each site, 10 *P. nigra* tree were selected, their diameter at breast height was measured, and they were sampled during multiple campaigns at midday, near the solar zenith.

3.1.1 | LWP

For each campaign, two green leaf shoots were collected for each of the trees and enclosed in aluminium sheets to maintain dark conditions until measurements in the lab. Then, shoots were kept in a cooling box for conservation before measuring LWP using a pressure chamber once back at the laboratory

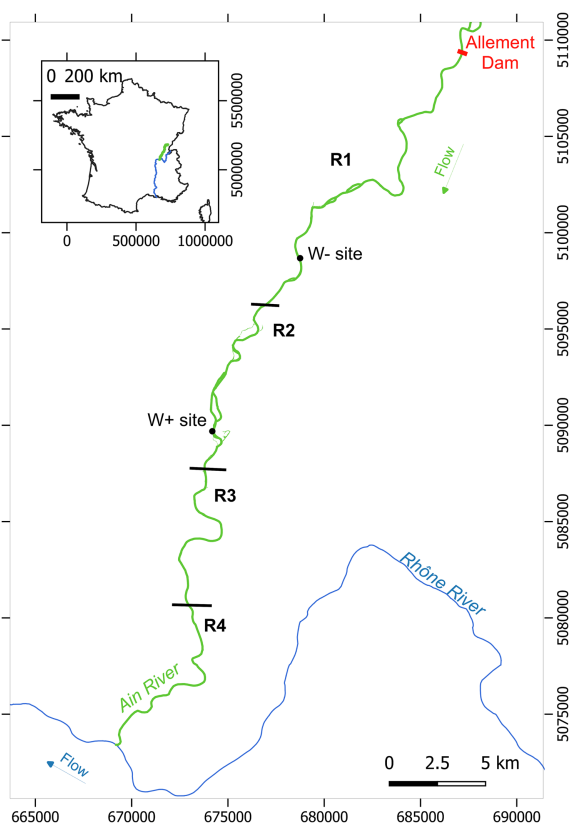


FIGURE 1 | Location of the lower Ain River and of the different study reaches. The coordinate system is EPSG 2154.

(Scholander et al. 1965). The leaf petiole was cut with a sharp blade and inserted in the pressure chamber. The mean pressure of the two selected leaves per tree was used as a single replicate.

During droughts, LWP is expected to decrease, with a stress threshold around -1.75 MPa having been previously identified for stomatal closure in *P. nigra* (Lambs et al. 2006).

3.1.2 | Phloem Collection and iWUE Calculation

Phloem of the trees was sampled every other field campaign and used to estimate the intrinsic iWUE of each tree according to the protocol published by Gerle et al. (2023), based on relative ratios in carbon isotopes in the phloem content (Vernay et al. 2020).

Briefly, phloem was collected with a bark corer (9 mm) at breast height in the trunk of each tree and immersed in 1.5 mL exudation solution (15 mM polyphosphate buffer: sodium hexametaphosphate, Sigma, München, Germany). Phloem was then removed from the tube before freezing the solution. The samples were then freeze-dried and rehydrated with deionized water in a tin capsule. After drying in an oven, the $^{13}\text{C}/^{12}\text{C}$ phloem ratio was analysed with a spectrometer and expressed in ‰ relative to Vienna Pee Dee Belemnite (VPDB).

Calculations to obtain iWUE are detailed in Gerle et al. (2023) and Vernay et al. (2020).

At the plant level, iWUE reflects the trade-offs between carbon intake and water use. Plants with high water use efficiency assimilate more C for the same amount of transpired water. During drought, iWUE values are expected to increase due to stomatal closure in response to heat stress or water stress: Plants respond to drought by reducing transpiration.

3.2 | Remote Sensing Data

3.2.1 | Airborne TIR Images

Images in the TIR spectrum (7.5–14 μm) were acquired in summer over four campaigns since 2010 (Table 2) with sensors mounted on an ultralight aircraft (2010 and 2022) or a helicopter (2011 and 2014). Three different sensors were used: a Thermo Tracer TH7800 for the first flight, a VarioCAM hr head for the second flight and a VarioCAM hr research 600 for the third and fourth flights. These cameras can detect

temperature differences of around 0.1°C within an image. Days of flight were chosen based on the weather and during low-flow conditions.

The images from the first three campaigns are historical TIR data available on the Ain River that originally aimed at studying river temperature to identify the inter-annual variability of cold-water patches. Therefore, the processing of these images is documented by the authors of the initial study (Wawrzyniak et al. 2016). The last airborne campaign was coordinated with the field campaign of this study (July 19), and the flight took place during the same timeframe.

3.2.2 | Satellite TIR Images

Landsat satellites were used as a source of coarse historical TIR data starting from 1990 by using Level 2 images from Landsat 5, 8 and 9. Images from Landsat 7 were not considered for the analysis due to the Scan Line Corrector failure that occurred in 2003. At most, one image was selected per year from the available data based on a rule of precipitation during the summer period (a 6-day window with no precipitation). This rule was defined according to results from preliminary analysis of airborne TIR data that showed the difficulty of assessing vegetation water stress from TIR imagery with wet antecedent conditions. This ensured that selected images were from the driest possible period for every summer.

3.3 | Additional Information for Geo-Referencing, Selecting and Characterizing the Study Area

Historical aerial photographs produced by the French Institut National de l'Information Géographique et Forestière (IGN) were used to provide information about land cover for dates close to the TIR campaigns. They were originally used by Wawrzyniak et al. (2016) to help manually geo-reference the TIR images. Aerial colour images were also acquired during the 2022 campaign by mounting a camera (Nikon Z6, 35 mm lens) on the aircraft during the TIR acquisition and were similarly used to assess land cover in 2022 and to help with the geo-referencing process.

Topo-bathymetric LiDAR data were acquired during August 2015 and covers the upstream half of the study reach (≈ 20 km), initially to study river bathymetry (Lague and Feldmann 2020). This dataset was then used to characterize the stationary conditions of the riparian forest in Godfroy et al. (2023). It is used in this study to help assess

TABLE 2 | Airborne TIR campaigns used in this study.

Date	Time	Spatial resolution (m)	Mean daily discharge ($\text{m}^3 \cdot \text{s}^{-1}$)	Daily maximum temperature ($^\circ\text{C}$)
30 July 2010	15:00 to 16:00	1.50	14.3	25.6
28 June 2011	17:45 to 18:30	0.70	13.4	34.0
3 July 2014	18:00 to 19:00	0.60	14.1	30.2
19 July 2022	12:20 to 13:30	0.35	16.2	37.1

the changes in canopy temperature based on forest stationary conditions.

The data were acquired with an Optech Titan sensor flown on an airplane and resulted in the acquisition of a point cloud with a final density of around 18.6 points per meter square for each of the two lasers of the sensor (green for bathymetry and NIR for above-ground) and with a mean vertical accuracy of ≈ 10 cm.

Vegetation surveys were conducted by ONF in 2007 and 2017 at the request of local stakeholders. It led to the survey of ~ 1200 forest plots in the study reach with the goal of providing extensive information on species distribution and health in the riparian forest of the Ain River, and, as such, one plot was assessed per hectare of forest. These vegetation plots were used to provide an extensive analysis grid common to the forest surveys and to previous studies (Godfroy et al. 2023) that covers the lower Ain River corridor. That grid is used for selecting forest patches within which Landsat TIR information is analysed.

Information about daily temperature and precipitations near the study site was accessed from the open access archives of the Ambérieu-en-Bugey meteorological station available from the Global Surface Summary of the Day (GSSD) provided by the National Centers for Environmental Information (cf. <https://www.ncei.noaa.gov/metadata/geoportal/>). Information on the flow level of the Ain River

was measured at the hydrological station located at Pont d'Ain and provided by the French Ministry of Ecological Transition (cf. <https://www.hydro.eaufrance.fr/>).

3.4 | General Workflow

Data analysis first focused on the campaign conducted during summer 2022 to investigate how the water status of *P. nigra* differed between the two study sites (Figure 2). Water status was assessed by monitoring changes in LWP and iWUE from field samples. Differences in LWP or iWUE between poplars and between sites were then assessed by running Student's test or Wilcoxon Mann-Whitney test depending on data distribution for each date. Differences between each week were assessed by using a pairwise *t*-test. Repeated measures ANOVA were then conducted to test the effects of environment (W+ and W-) and time on LWP and iWUE values (environment, time and their interaction were used as explanatory variables in the ANOVAs). Meteorological data from the start of the campaign to its end were then plotted to recontextualize the observed trends in water stress with the trends in air temperature and precipitations of summer 2022.

TIR data from 2022 were then analysed by first looking at differences in tree crown temperature between poplars from the two sites. In order to retrieve tree crown temperature, the shape of each tree crown was first delineated manually by combining

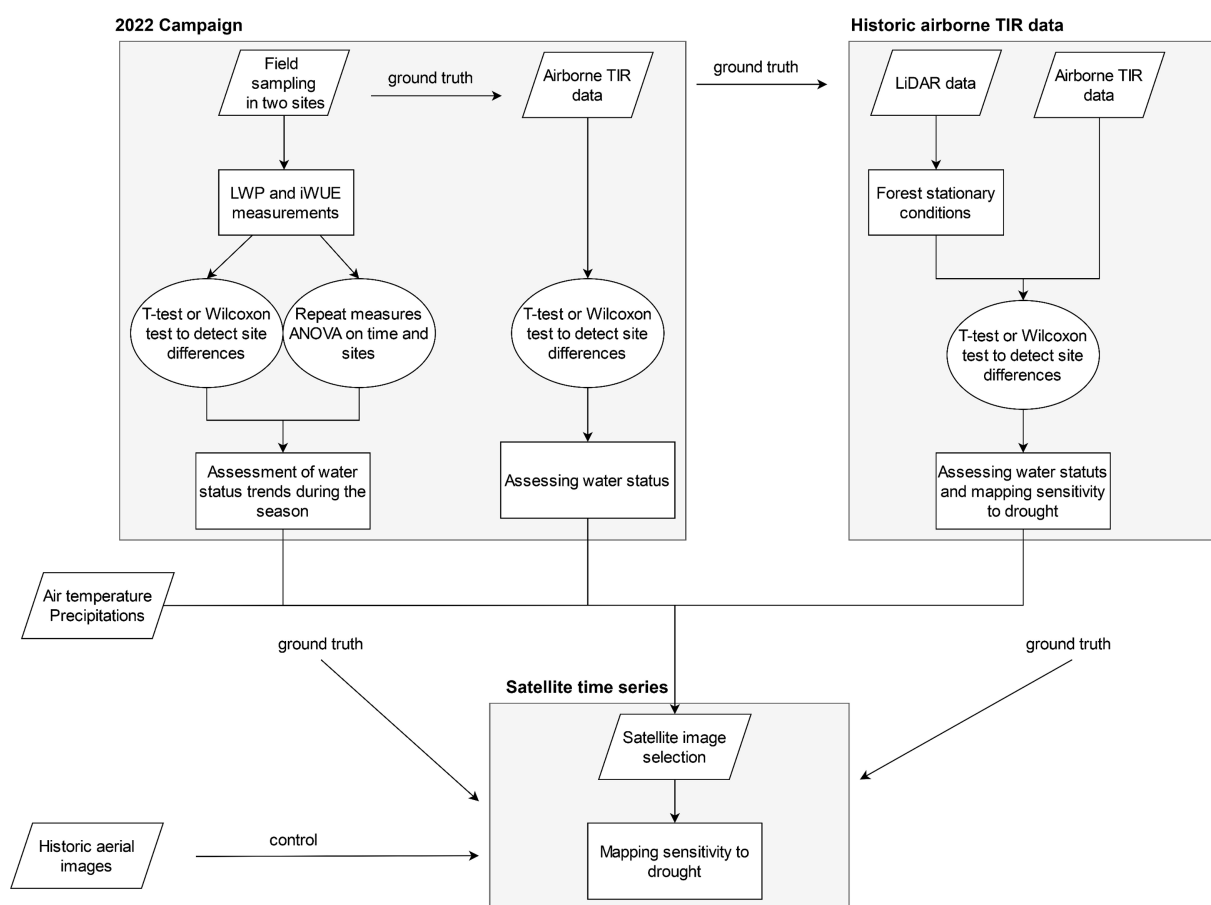


FIGURE 2 | General workflow of our study.

GPS positions of each tree with the aerial images synchronous to the TIR acquisition and canopy height extracted from the LiDAR dataset. Median temperature was then extracted for each tree crown from TIR data. Differences between the poplars on the two sites were then assessed using the same tests as for LWP and iWUE.

Tree diameter from the field survey and tree height from the LiDAR data were tested to predict LWP, iWUE and TIR as potential variables to explain differences between individuals on a given site for all dates during summer 2022 for which data were available.

Data analysis then focused on using existing airborne TIR imagery to detect water stress and map the sensitivity of the riparian forest to drought. The relationship between canopy temperature and stationary conditions at the level of forest plots was investigated for all four campaigns.

In order to retrieve information on canopy temperature for each forestry plots, the closest aerial images available to each campaign were used to screen forest plots and mask areas that were not vegetated. The 90% percentile (D90) of canopy temperatures was then extracted in each plot in order to minimize effects from shadowing.

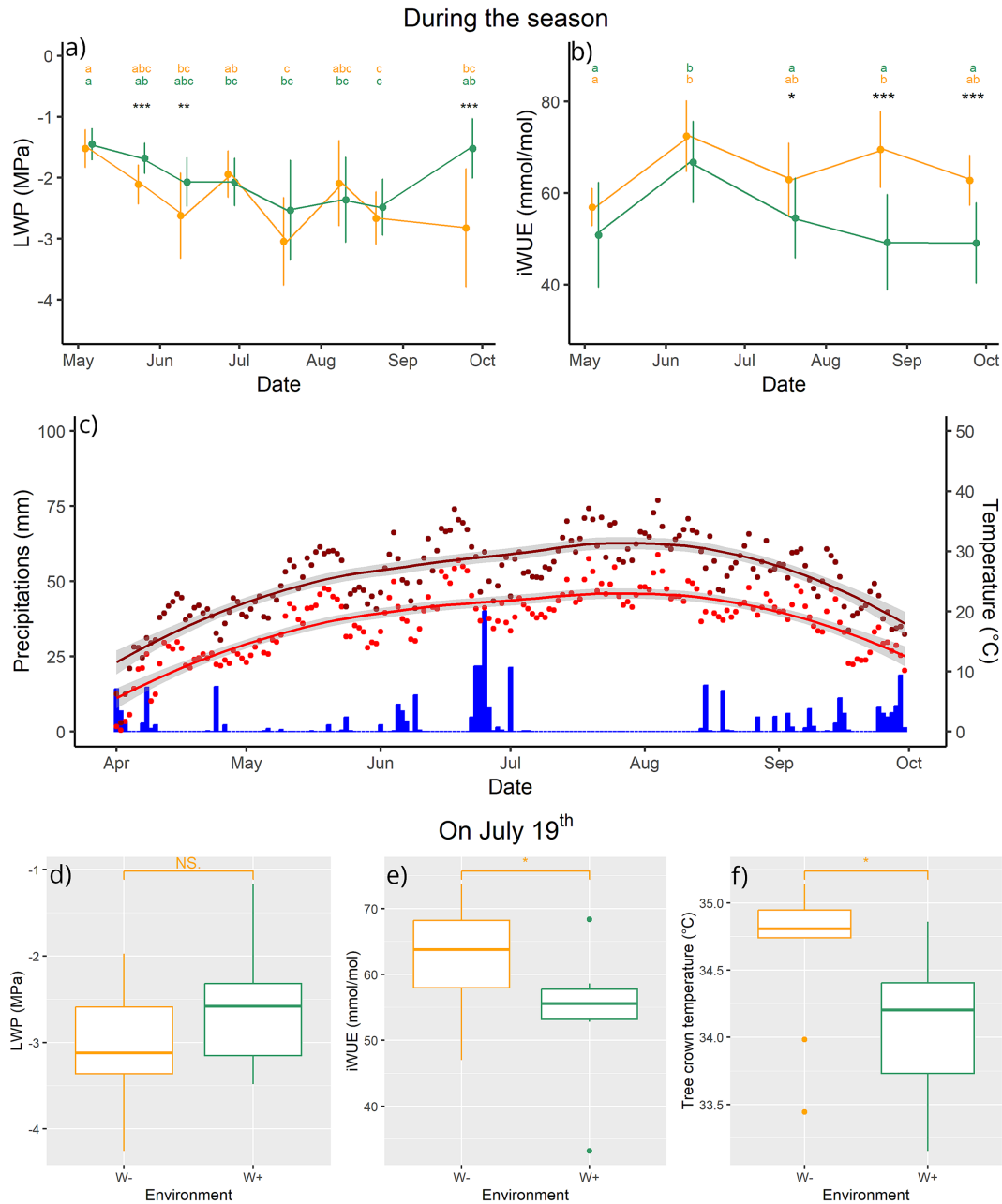


FIGURE 3 | (a) Leaf water potential (LWP) and (b) intrinsic water use efficiency (iWUE) on the W+ site (green) and W- site (orange) and (c) precipitations (blue) and daily mean (red) and daily maximum (dark red) temperatures for the study period; (d) leaf water potential, (e) intrinsic water use efficiency and (f) tree crown temperature depending on the study site on July 19, 2022. Stars indicate differences in LWP or iWUE between the two sites (Wilcoxon or Student's tests depending on data distribution, * $p < 0.05$, ** $p < 0.001$, *** $p < 0.001$), and letters indicate the differences between dates from pairwise t -tests.

Stationary conditions were assessed by detrending LiDAR-derived DEM using the Fluvial Corridor Toolbox (Roux et al. 2015). This detrended DEM was obtained by subtracting the elevation of the water level of the river from the elevation of the terrestrial floodplain level, resulting in values of elevation relative to the water level under low-flow conditions ($Q = 16 \text{ m}^3 \cdot \text{s}^{-1}$). The mean value from the detrended DEM was then extracted for all forest plots in the coverage of the LiDAR data and used to create two classes of stationary conditions based on previous literature on the Ain River (Dufour and Piégay 2008; Godfroy et al. 2023), with a 'good connectivity' class for plots lower than 2.5 m above low flow and a 'disconnected' class for plots 2.5 m above low flow and higher.

The same methodology as for the analysis of the 2022 data was then applied by running Student's test or Wilcoxon Mann-Whitney test depending on data distribution for each campaign in order to detect differences in canopy temperature due to stationary conditions. The campaign from 2022 was used as a control of the expected response in temperature canopy under known stress conditions, and hydrological and meteorological data for the week before the campaign were plotted to contextualize the observations.

Maps of riparian forest sensitivity to drought were then produced using relevant campaigns. In order for maps to be comparable despite differences in atmospheric conditions at the time of survey, canopy temperature values were discretized using quartile statistics.

Similar maps were then created using Landsat data to highlight lasting changes since 1990. Image selection is described in Section 3.2.2. At-sensor resolution (100–120 m) was higher than the spatial footprint of the forest plots (20 m radius, with 100 m between plot centers), so mean temperature was extracted for each plot, and a map was produced to help assess and discuss the impact of the original footprint of the sensor on the results by using available orthophotos.

4 | Results

4.1 | Field Validation of Tree Water Stress and TIR Response

Field surveys show that the water status of poplar trees varies during the summer period. In particular, both sites reached stress conditions during summer as LWP values were generally lower than -1.75 MPa from June to September (Figure 3a).

LWP values at the connected site (W+, in green) decreased until reaching a plateau near -2.5 MPa starting from the middle of June before increasing back to -1.5 MPa at the end of September. For the disconnected site (W-, in orange), LWP decreased faster than for the connected site, reaching values near -3 MPa on average in July. A more contrasted recovery is observed for

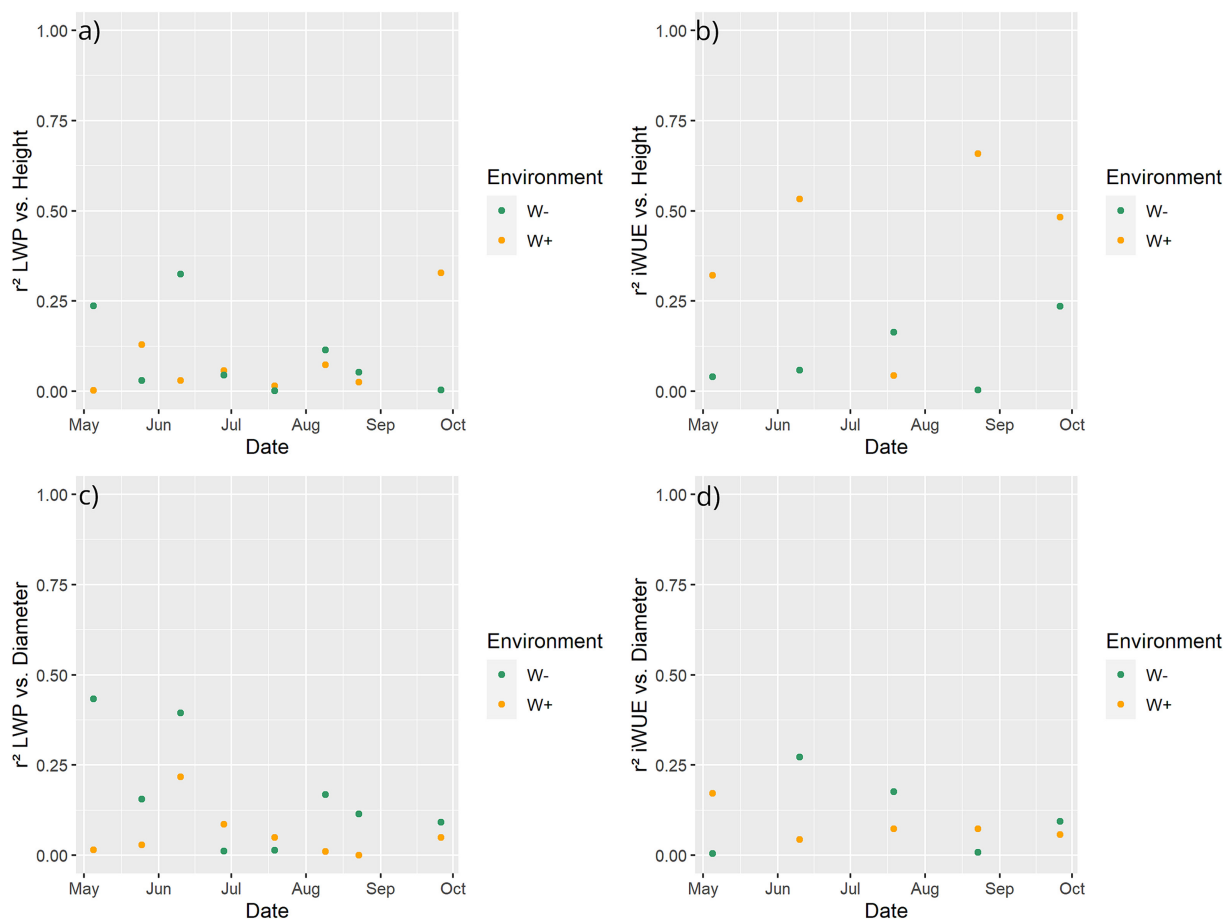


FIGURE 4 | r^2 of the linear relationship between (a) LWP and tree height, (b) iWUE and tree height, (c) LWP and tree diameter and (d) iWUE and tree diameter for each sampling date and site.

these poplars as LWP values at the end of September were still around -3 MPa on average, but variability between individuals increased, which suggests partial recovery. In addition, LWP values were more variable for poplars on the disconnected site with short recovery periods (June 28 and August 9) where mean LWP values were closer to that of the connected site. Differences between sites were most significant at the beginning of the stress period when LWP values increased with each subsequent campaign (May 25 and June 10) and at the end of September (September 26) after which the connected site fully benefits from the recovery period.

Although iWUE measurements were sparser and notably not conducted on June 28 or August 9 (dates for which LWP values fluctuated for the disconnected site), they show a trend similar to LWP measurements (Figure 3b). An increase in iWUE values was observed for both sites during summer, from 40 to 45 mmol/mol and reaching values near 50 mmol/mol and 60 mmol/mol on average for the connected and disconnected sites, respectively. This is in line with trees in both the connected and disconnected sites displaying low LWP under the threshold considered as a water stress response. Water stress may certainly induce a stomatal closure to reduce transpiration, increasing iWUE. A recovery period is identified at the

end of summer, with decreasing iWUE values starting August 23 for the connected site and at the end of September for the disconnected site. Although iWUE values were on average higher for poplars in the disconnected site, differences between the two sites were significant during summer (July 19 and August 23) and at the end of September.

The ANOVA tests performed on repeated measures indicated a significant effect of the environment (W+ vs. W-, $p=0.017$, $F=8.583$), of the week of the sampling ($p < 10^{-3}$, $F=10.034$) and of the environment \times week interaction ($p < 10^{-3}$, $F=4.413$) on LWP. For iWUE, only an effect of the week ($p < 10^{-3}$, $F=15.625$) and of the environment \times week interaction ($p < 10^{-3}$, $F=3.412$) were significant, but not the effect of the environment alone ($p=0.099$, $F=4.091$).

Those two indicators converge towards an increasing water stress in *P. nigra* during summer and a recovery in late August or during September, which follows temperature and rainfall trends for summer 2022 (Figure 3c).

Tree sampling and TIR data were acquired simultaneously on July 19, which means all three indicators of water stress can be compared for the disconnected (W-, in orange) and connected

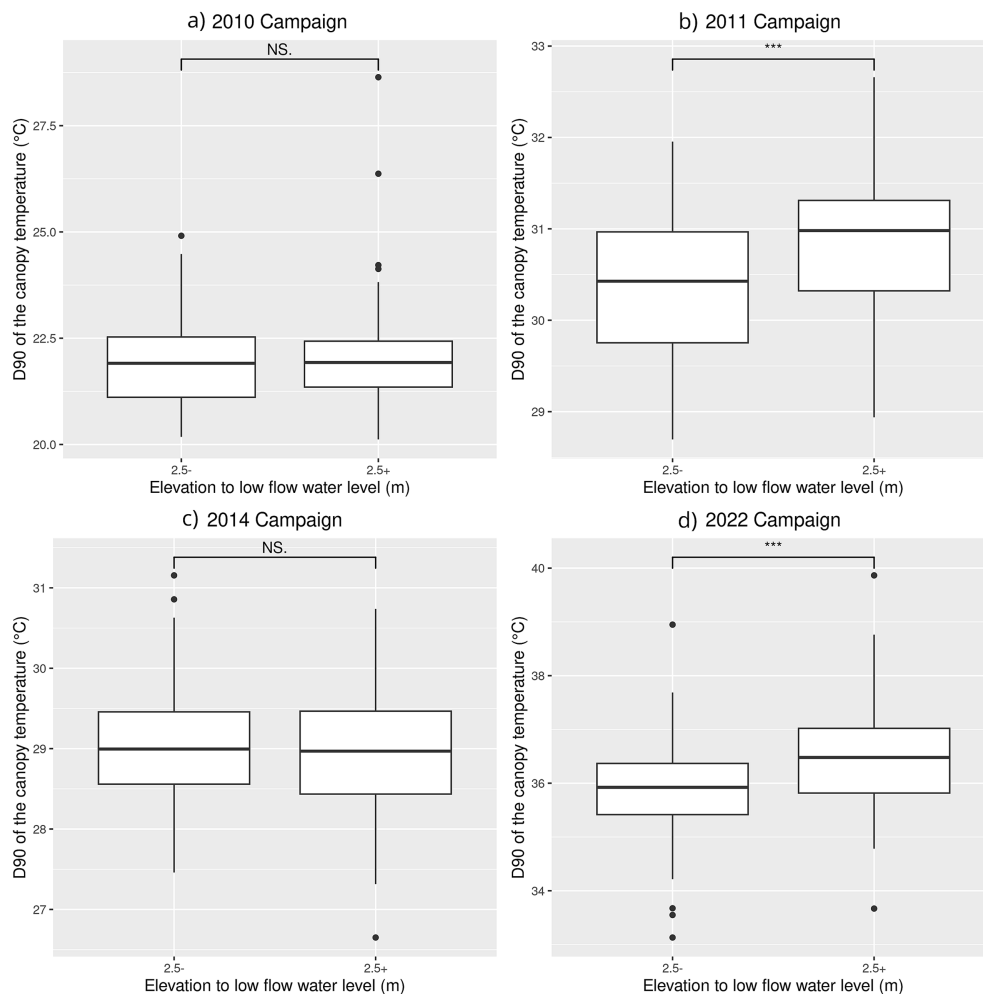


FIGURE 5 | 90% percentile of canopy temperature at the plot level depending on plot elevation to low-flow water level for all four airborne TIR campaigns: (a) 2010, (b) 2011, (c) 2014 and (d) 2022. Stars indicate the differences between plots (results from Wilcoxon or Student's tests depending on data distribution, * $p < 0.05$, ** $p < 0.001$, *** $p < 0.001$).

(W+, in green) sites for the same date. On this date, LWP values were lower in the disconnected site than in the connected site (Figure 3d), and the opposite was true for iWUE values (Figure 3e). However, these differences were only significant for iWUE ($p < 0.05$). This validates a higher stress status in the disconnected site. Canopy temperature of sampled trees was higher in the disconnected site ($p < 0.05$) which also suggests higher water stress for poplars in the disconnected site (Figure 3f).

The relationship between tree physiognomy and the three indicators of water stress was also investigated (Figure 4). Although r^2 values were low for most of the dates, intra-seasonal variability was also recorded. Higher r^2 values were reached for LWP at the beginning of summer for trees in the disconnected site (from 0.25 to 0.50) and for iWUE at the beginning and the end of the summer for trees in the connected site (from 0.25 to 0.70). The relationship between canopy temperature and tree height or tree diameter also reached high r^2 values for the trees at the disconnected site (0.55 and 0.60, respectively). Overall, when a high r^2 value was recorded, bigger trees (higher diameter or height) were less stressed (higher LWP, lower iWUE and lower canopy temperatures) than smaller ones.

4.2 | Inter-annual Differences in Airborne TIR Response to Summer Conditions

In the absence of in situ assessment of the water status of the riparian forest for the historical airborne surveys, only the thermal response of riparian vegetation to differences in connectivity can be assessed. Using a breakpoint value of 2.5 m above the low-flow water level as the main variable to consider shifts in connectivity, the results from an analysis at the plot level in 2022 were similar to those of the analysis at the level of individual tree crowns (Figure 5).

Indeed, in 2022 (Figure 5d), canopy temperatures were higher for plots with higher elevation to the water table ($p < 0.001$), which is similar to the higher crown temperatures for trees in the disconnected site. Although this was also true for the 2011 (Figure 5b) campaign ($p < 0.001$), there were no differences in canopy temperature between the two classes of stationary conditions (connected for plots where elevation to low flow is < 2.5 m and disconnected for plots where it is > 2.5 m) for 2010 (Figure 5a) and 2014 (Figure 5c). These results highlight the sensitivity of the thermal response of riparian vegetation to hydrometeorological conditions before and on the day of data collection. Observing a thermal response to tree stationary conditions (i.e., a difference in the ability of trees to evapotranspire and cool their canopy) for 2 years but not the others suggest that trees were not water limited during all acquisition windows.

4.3 | Mapping of Airborne TIR Responses to Summer Droughts: 2011 vs. 2022

The statistical distribution of canopy temperatures was mapped for 2011 and 2022 using quartiles (Figure 6a), and a confrontation of the two maps (keeping only forest plots for which thermal

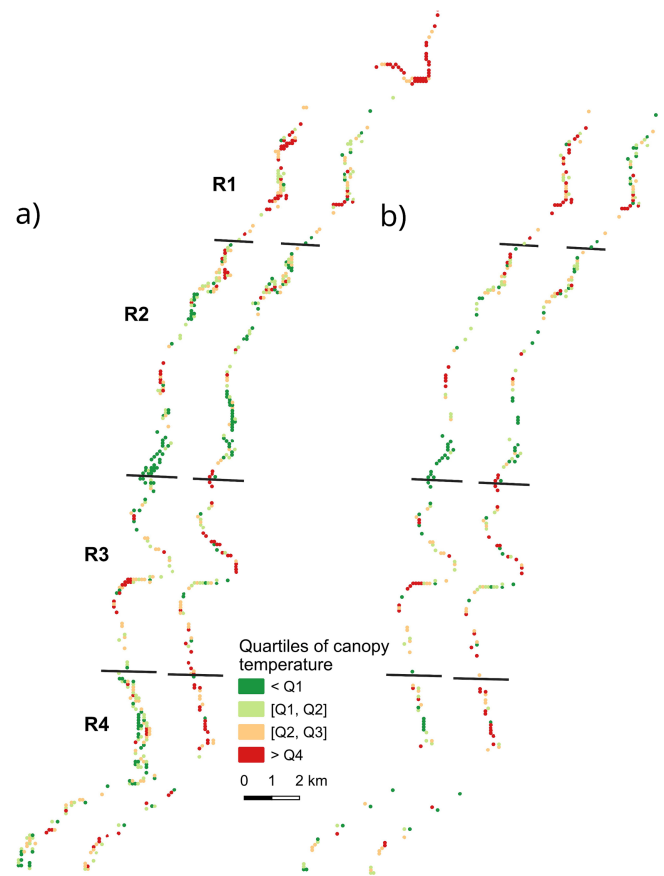


FIGURE 6 | (a) Spatial distribution of the different quartiles of canopy temperature in 2011 and 2022 for all ONF plots and (b) a 2011–2022 comparison using only plots for which data was available both in 2011 and 2022.

information was available in both 2011 and 2022) is shown Figure 6b.

Both acquisitions covered most of the riparian corridor near the main channel of the Ain River and poorly covered larger areas of riparian forest that were created by river meandering. The higher canopy temperatures were concentrated in the R1 and R3 reaches, whereas the lower canopy temperatures are located in the R2 and R4 reaches. As R1 was the most geomorphologically degraded reach suffering from historic channel incision and R2 was the most geomorphologically stable reach, the spatial distribution of canopy temperature suggests that the health of the riparian forest and its sensitivity to drought reflect 20th century change in geomorphology.

Figure 6b highlights changes in the distribution of canopy temperatures between 2011 and 2022 by keeping only forest plots with thermal information available for both periods. Changes mainly occurred in the R1 and R4 reaches. Although forest plots with higher canopy temperatures were mainly located in the R1 reach in 2011, the distribution of canopy temperature in 2022 suggests partial recovery following restoration work in the reach. On the other hand, the opposite trend is visible for forest plots in reach R4.

4.4 | Mapping Large-Scale Riparian Thermal Changes Using Landsat Archives

Based on the results from field validation, selection of TIR Landsat data was constrained by precipitation (no rain during a 6-day period preceding observations from 2011 and 2022) and by cloud cover (visually inspecting each image). With one image selected per year at a maximum, this resulted in only 14 images selected for the 1990–2022 period. The resulting maps also compared the distribution of temperature quartiles for each year but used all available forest plots due to the higher spatial extent of satellite data (Figure 7).

The spatial distribution of canopy temperature quartiles was very similar for each year satellite data were available. Plots showing higher temperature were mainly distributed in the R1, R3 and R4 reaches, with most of the plots in the R2 reach being consistently among the coolest plots. Lower temperatures also feature plots

near the confluence with the Rhône River, in the middle section of the R3 reach since the start of the new century, and plots near the main channel or in the upstream-most section of reach R1.

Although the resolution of satellite thermal data is coarse, strong and meaningful change is still highlighted in the area near the confluence with the Rhône River that is of interest to understand forest dynamics in regard to meteorological and geomorphic constraints (Figure 8).

On the aerial images, a simplification of channel morphology towards a lower active channel width is visible between 1995 and 2001 and illustrates the geomorphic changes that occurred at the end of the century in this section of the lower Ain River valley. In the case of the riparian forest, canopy temperature progressively increased relative to the rest of the lower Ain River valley between 2000 and 2005 leading to a shift from lower quartiles of temperature to higher quartiles of temperature. This shift

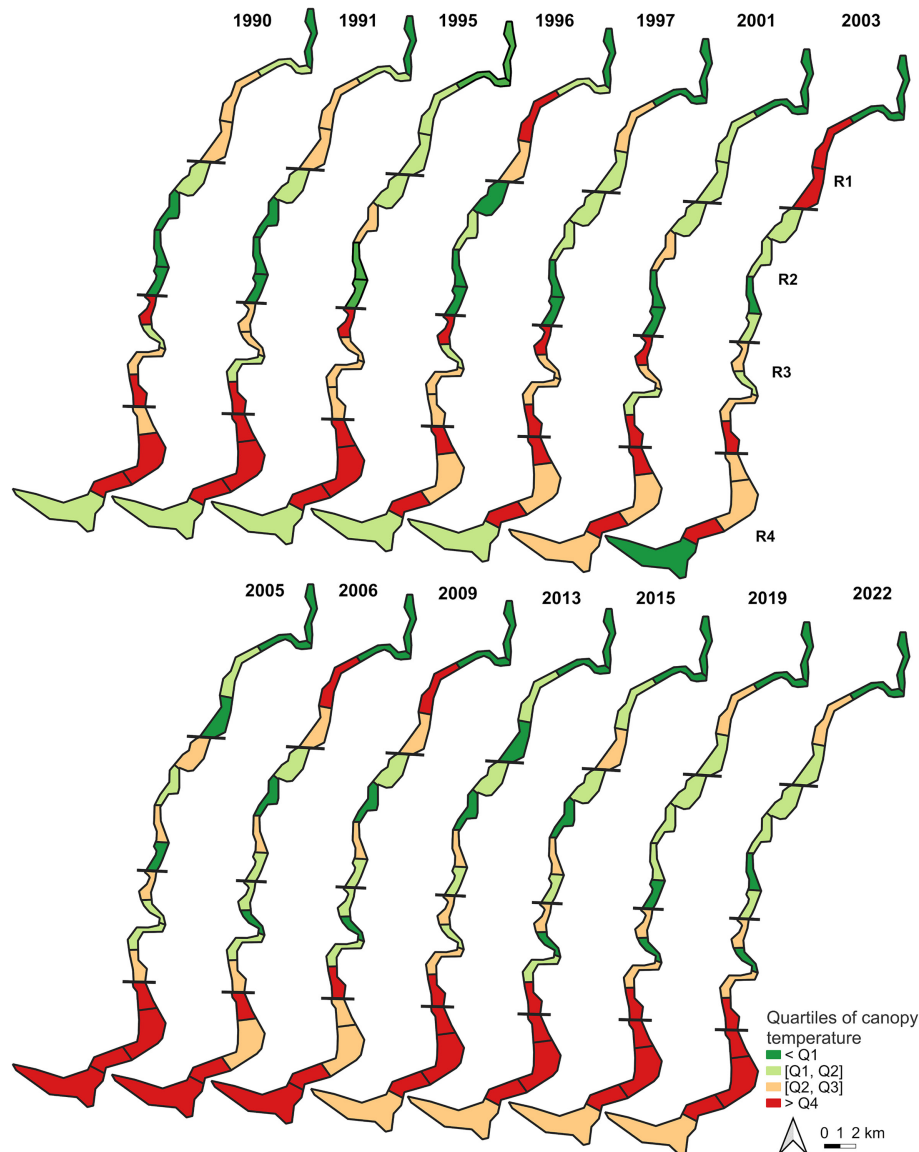


FIGURE 7 | Spatial distribution of canopy temperature quartiles at the corridor scale from Landsat data between 1990 and 2022. Each reach was subdivided in four sectors of similar river length and the information for each forest plot was summarized for each sector to facilitate reading.

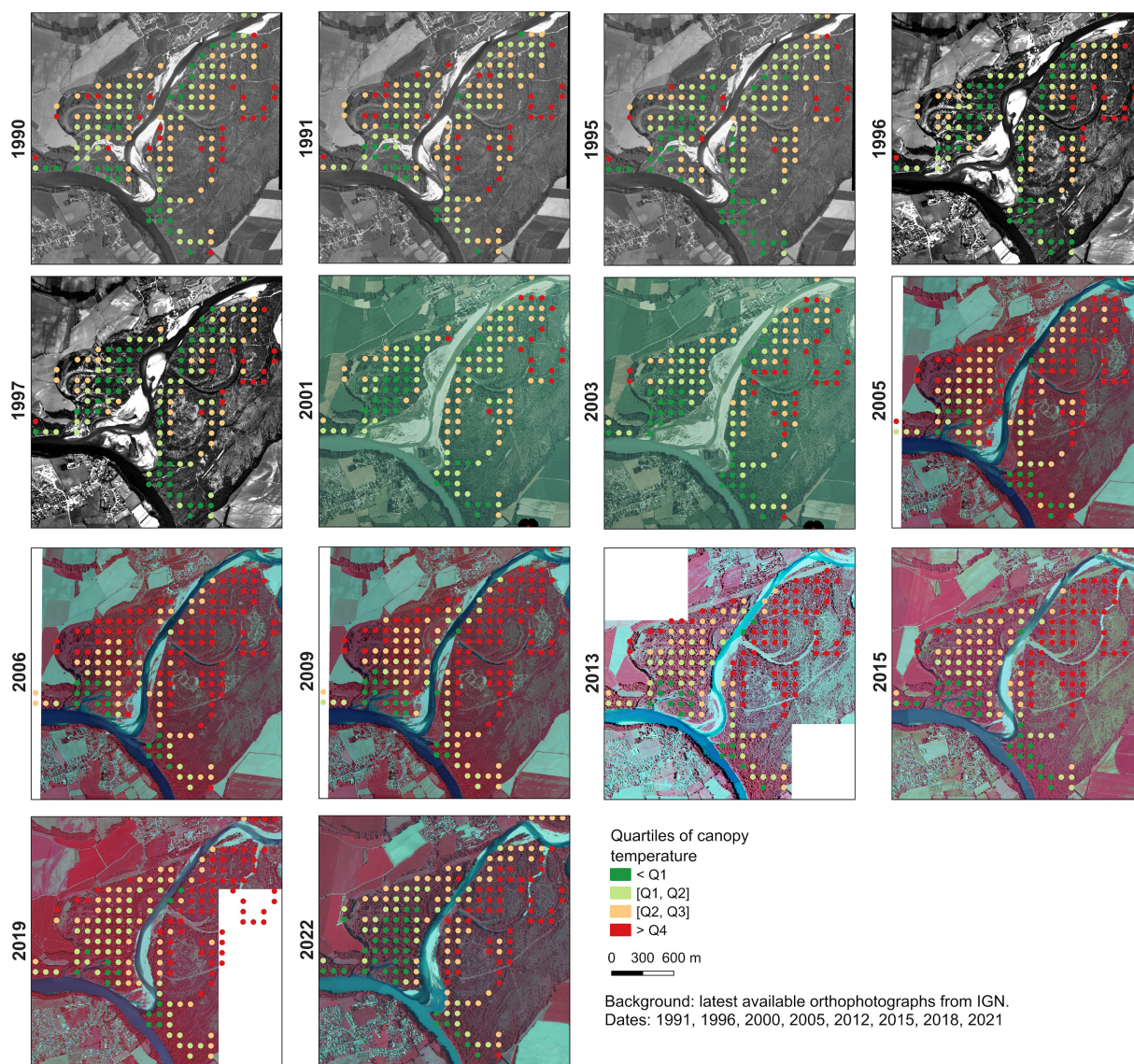


FIGURE 8 | Evolution of the sector at the confluence with the Rhône River since 1990.

is more pronounced on the left side of the river as the right side appears to have recovered by 2022.

5 | Discussion

5.1 | Summer Water Stress Conditions of Poplar Trees Depend on Water Accessibility

Our results suggest that the water stress conditions of riparian poplars depend on water accessibility. Differences in the health status of trees were observed for all indicators (tree crown temperature, LWP and iWUE), showing the contrasted response of *P. nigra* to drought based on its stationary conditions. The trees from the dryer site were consistently showing higher water stress on one or more of the indicators used in this study, compared to trees from the wetter site.

When considering a stress threshold at -1.75 MPa value for the LWP, as reported for *P. nigra* stomatal closure in previous

studies along the Drac and Isère rivers (Lambs et al. 2006), stress conditions were reached for poplar individuals in summer 2022 regardless of their stationary conditions. Although trees in more connected reaches of the river were displaying lower stress according to the indicators (higher LWP, lower iWUE and lower canopy temperature), they still experienced water scarcity. Therefore, the threat of drought-induced changes in riparian forests can even affect river reaches with good geomorphic conditions and be exacerbated in river reaches where anthropogenic activity has already historically altered water accessibility.

Such a change following a drought event was recorded in this study. Long-term change analysis based on Landsat archives showed a shift in the riparian forest health status near the confluence with the Rhône River. The timing of this change corresponds to the hottest and driest summer recorded in France: the 2003 drought (Black et al. 2004; Luterbacher et al. 2004). The fact that satellite data were able to detect such a change despite its coarse pixel resolution suggests that the shift in forest structure is significant, with a more open canopy, and a

temperature measurement at sensor mixing the signals from the canopy, the understory and potentially even the forest ground. This would be consistent with the field surveys by ONF noticing a higher number of dead poplars in this sector and that they attributed to that summer 2003 drought. Similar vegetation dieback has been recorded using remote sensing data in other river systems following drought events (e.g., Kibler et al. 2021).

Tree response to stress however may vary. Although tree mortality and the decline of the poplar forest is one of the possible responses to stress, it is not the only one. Water scarcity can also impact tree growth and lead to changes in productivity of riparian trees (Lambs et al. 2006; Monclus et al. 2006; Smith et al. 1991) and therefore impact both the ability of trees to act as carbon sinks and their structure (e.g., diameter, height and leaf size). Specifically, for *P. nigra*, plasticity has been shown across a range of climatic conditions in Europe, with individuals from certain locations (e.g., Spain) being more adapted to drier environments by having slower growth with smaller leaves and a faster stomatal closure (Viger et al. 2016).

In our study, the relationships between tree height or diameter and several indicators were tested but were only significant for a few dates. Trees on the disconnected site with a larger diameter had higher LWP at the beginning of the stress period and lower canopy temperatures during the TIR acquisition. On the other hand, trees from the connected site with a higher tree height had a better recovery at the end of the summer. Interestingly, the allometric relationship between tree height and tree diameter was distinct for the two sites (see Figure A1). This highlights how water scarcity, albeit due to channel incision (Godfroy et al. 2023; Rollet et al. 2014), has already affected tree physiognomy in our study reach and may explain the observed differences in tree response along the height–diameter gradient between sites. Indeed, smaller trees are similar, but differences in height-to-diameter ratios are observed when trees grow larger.

In addition, not all historic airborne TIR data were collected under stressful conditions, as only two campaigns showed changes in canopy temperature based on the vertical connectivity of forest plot. Lower temperatures and higher precipitations before the two other campaigns (Figure A2) may not have led to stress conditions. Although our number of observations was too low to be significant, the meteorological conditions in a 3-day time period before the campaign were strongly correlated to TIR-derived stress indicators (Figure A3). This is also supported by the intra-seasonal variability of the stress signal as measured by the LWP of the poplar trees that showed a partial recovery for dates sampled following rainfall events.

This shows that identifying the role played by water accessibility in the response of riparian forests to drought is difficult because it related to both river-related dynamics (such as access to groundwater following channel incision or depending on flows during summer) and meteorological dynamics (such as precipitations temporarily replenishing water content). In addition, although we studied *P. nigra* as it is a phreatophyte species, other species in the riparian forest such as *F. excelsior* do not have the same root systems and are limited to the vadose zone for accessing water resources (Dufour 2005).

5.2 | The Benefits of a Multi-tool Approach to Understand Tree Response to Water Stress

Our results also shed light on the tools available to assess and monitor water stress in riparian forests. One of our main findings in regard to the study design is that all our indicators were sensitive to acquisition timing and did not always detect differences in stress intensity based on forest stationary conditions, making it difficult to assess the stress status of the forest or individual trees.

In-field sampling was used successfully to detect the occurrence of water stress from May to September, and both LWP and iWUE showed an expected increase in stress intensity during the summer. On the other hand, although both indicators detected differences between individuals from the two sites, the dates for which results were the most significant did not match except during the recovery period at the end of September.

Similarly, using airborne TIR data did not yield relevant results for all of the dates data were available. Due to a lack of historic in situ assessment of tree water status, it is not possible to know if stress conditions would have been reported using another indicator. However, these results show that the ideal acquisition window for studying vegetation health using thermal data is not the same as the ideal acquisition window to study river temperature (i.e., the aim of the initial historical study): Data to study interactions between the river and groundwater (Wawrzyniak et al. 2016) do not always provide accurate information on vegetation status. However, it also means that having such wider implications in mind when planning data collection can help optimize efforts and resources in making data relevant beyond its original use.

Considering ground truth, a careful study design based on antecedent hydro-climatic conditions and a deep knowledge of geomorphic conditions in a river corridor seem crucial to studies seeking to employ airborne TIR imagery to assess water stress.

However, some level of variability is to be expected because different indicators of water stress do not correspond to the same biophysical processes and might not share the same response time to environmental variables (Volaire 2018), and water stress progresses from the upper shoots in the tree crown to the tree trunk and the roots (Lambs et al. 2006).

For example, stomatal closure, which has been linked to changes in transpiration and an increase in leaf temperature (Hsiao and Acevedo 1974; Jones 1999), occurs slowly over a range of LWP depending on the rate of stress (Jones and Rawson 1979). In *P. nigra*, higher rates of stomatal closure were related to higher iWUE (Viger et al. 2016). After rewatering, the reopening of stomata lags behind recovery in LWP, and the duration of this lag is dependent on the degree of water stress and the species considered (Liang and Zhang 1999). This is consistent with our observations of a delay between stress measured through LWP and the increase in iWUE.

Overall, multi-tool monitoring would allow to better understand the stress signal of the riparian forests in their natural conditions and the delays between the responses that can be

measured at the canopy level with remote sensing and the events leading to stress conditions. Additionally, using optical indexes or LiDAR data to retrieve parameters such as canopy greenness and structure would also allow us to better understand under which conditions the stress experienced by riparian trees leads to responses such as leaves yellowing, biomass loss and reduced growth.

5.3 | Good Practices in Designing Campaigns to Monitor Water Stress in Riparian Ecosystems

Based on this information and our results, designing campaigns to assess or monitor water stress in riparian environment at large scales should couple TIR acquisitions with complementary data to cross-validate the observations such as in situ measurements of water stress at target sites and optical remote sensing indexes. Acquisitions would need to be planned depending on when the stress is expected to occur, the lag in response for the indicators used and their sensitivity to other environmental variables. Under these conditions, multi-date surveys are recommended to obtain multiple observations for a given summer. Our results also show that the acquisition of TIR data should target the peak of the stress period and avoid dates with recent precipitations that could replenish water resources and affect air humidity.

Another way to acquire TIR data would then be to rely on drones or satellites as other airborne vectors such as helicopters or airplanes are less flexible in regard to the time of acquisition and are more costly, which limits both the ability to acquire data multiple times per season and to target the most optimal window for TIR sensing of vegetation health. However, the use of satellite TIR data is limited by the poor spatial resolution of current TIR sensor, which impacts their applicability to an early detection of water stress as they may be more sensitive to more delayed responses to stress conditions such as changes in canopy structure due to vegetation dieback and shifts in communities. Drone acquisitions suffer from lower spatial extent, but the technology is emerging for the study of river temperature (Dugdale, Klaus, and Hannah 2022; Redana et al. 2024) after initial low-cost sensors proved prone to temperature drifting (Dugdale et al. 2019). They would however provide the high temporal resolution needed to better study how canopy temperature can be used as an indicator of water stress in complex and heterogeneous riparian environments by coupling drone acquisitions with in situ surveys like those conducted in this study.

Multi-scale acquisition could help answer some of these issues by providing higher resolution data as ground truth, which is increasingly common when processing satellite data (Carbonneau et al. 2020), or by using repeated drone surveys to help identify when more costly airborne acquisitions over a larger spatial extent should be conducted.

5.4 | Production of Spatially Explicit Knowledge for Stakeholders and River Management

The results in this study builds upon previous research by validating the hypothesis that the riparian forest of the Ain River experiences water stress in the summer. Previous

studies focused on an upstream–downstream gradient (Lejot et al. 2011) or on stationary conditions (Dufour 2005; Godfroy et al. 2023; Rollet et al. 2014) to highlight differences in the health status of the riparian forest but did not directly approach water stress issues. Here, we were able to confirm the presence of water stress during the summer using ecophysiological in situ measurement. We then discovered that water stress conditions impacted *P. nigra* individuals in areas where we expected an unstressful water availability, shedding light on the fact that even better connected sectors of the riparian forest were experiencing water stress during summer 2022.

By applying an approach previously known to have an impact on the growth of *F. excelsior* (Dufour 2005) and on the distribution of species in the riparian forest and its structure (Godfroy et al. 2023), focused on stationary conditions, we also detected a direct effect of stationary conditions on the stress status of *P. nigra*. Drier stationary conditions due to channel incision led to higher levels of water stress during summer, and surveyed poplar trees experienced stress conditions earlier than those in reaches in better geomorphic conditions. These results support previous studies on other river systems that linked channel incision with an increase in mortality due to stress (Scott, Lines, and Auble 2000).

Although in situ assessments of the water status focused on *P. nigra* because it was both the dominant species in the Ain River valley and of interest to local stakeholders, other riparian species might respond differently to droughts as previously described in Section 5.1. This could limit results' reproducibility and interpretability, yet in our study, the relationship between forest stationary conditions and canopy temperature from airborne sensors held true at both the level of individual tree crowns and forest plots.

Overall, our results show that acquiring and using TIR data at various spatial scales can help monitor the health status of riparian forests and their response to anthropic pressures to generate actionable information for river managers.

In our case, we were able to detect a higher sensitivity of the riparian forest in Reach R4 to the 2003 drought, which may partly be explained by lower water access compared to Reach R2 and by more pioneer populations compared to reaches R1 and R3. Because protecting pioneer environments is one of the priorities of local stakeholders, our results indicate that current gravel reinjection actions that focus on reaches R1 and R2 might not be sufficient to protect riparian environments closer to the confluence with the Rhône River from drought. In order to reduce the impact of climate change and warming weather on riparian forest, gravel reinjections actions closer to this sector could be considered to limit channel straightening and incision and improve groundwater access for pioneer trees. In a social context where the construction of a dam on the Rhône River upstream the Ain–Rhône confluence is being discussed, careful consideration needs to be given to the already fragilized riparian forest in this sector as this could exacerbate water stress issues and contribute to a shift towards drier communities to the detriment of pioneer species such as *P. nigra*.

6 | Conclusion

Water stress conditions were detected using in situ measurements and showed increased water stress on black poplars located in dryer terrestrial river margins. Airborne TIR remote sensing was able to detect this difference in water status due to an increase in canopy temperature and enabled mapping of the riparian forest response to drought events on a 50-km reach of the Ain River. Differences in the spatial distribution of forest sensitivity over a 10-year period highlighted forest degradation in one of the reaches and provided feedback on current restoration efforts. The use of satellite TIR data was investigated, but due to coarse spatial resolution and the limited spatial extent of riparian corridors, observations were more likely related to larger scale canopy openness and proximity to other land covers rather than water status, therefore highlighting the need for further studies coupling satellite data with ground truth acquired at higher resolution. Nonetheless, lasting degradations were detected near the confluence of the Ain River with the Rhône River, which can be attributed to the combined effects of the 2003 drought event and groundwater levels lowering caused by channel incision. However, the variation of the stress signal during summer and the fact that not all surveys showed a temperature effect on tree canopy related to drought show the importance of multi-date and multi-source surveys when attempting to assess or monitor water stress in complex heterogeneous environments such as riparian forests. Despite these requirements, airborne TIR mapping appears as a promising tool to monitor the response of river systems to climate change thanks to its ability to inform about the water status of the riparian forest and to additionally provide crucial information about other components of river systems such as water surface temperature, but it needs to be repeated over the seasons and years to detect long term effects of such potential ramp disturbance (e.g., cumulative effects of heat pulses that are supposed to be more frequent and more intense).

Author Contributions

Julien Godfroy: conceptualization, methodology, formal analysis, investigation, data curation, writing – original draft, writing – review and editing. **Pauline Malherbe:** formal analysis, data curation, writing – review and editing. **Flavie Gerle:** formal analysis, data curation, writing – review and editing. **Baptiste Marteau:** investigation, methodology, data curation, writing – review and editing. **Pierre Lochin:** investigation, data curation, writing – review and editing. **Sara Pujalon:** writing – review and editing, supervision. **Jérôme Lejot:** writing – review and editing, supervision. **Antoine Vernay:** conceptualization, formal analysis, investigation, data curation, writing – review and editing, supervision, funding acquisition. **Hervé Piégay:** conceptualization, methodology, writing – review and editing, supervision, funding acquisition.

Acknowledgements

This research was funded with the support of the Graduate School H2O Lyon (ANR-17-EURE-0018) of the Université of Lyon (UdL), which is part of the programme 'Investissements d'Avenir' operated by Agence Nationale de la Recherche (ANR). This work was also carried out within the framework of the Fédération de Recherche BioEEnViS. The work of Julien Godfroy was also supported by the Agence de l'Eau Rhône Méditerranée Corse. The work of Pierre Lochin was supported by the Graduate School H2O Lyon and by the US National Science Foundation (EAR 1700517 and EAR 1700555). Baptiste Marteau's contribution was partly funded through the national 'Plan de Relance' programme

coordinated by ANR. The authors would like to thank Kristell Michel and Christelle Boisselet that contributed to study design and lab work. They also want to thank EDF and Dimitri Lague from the Université de Rennes (UMR 6118) for the topo-bathymetric LiDAR data. Finally, they wish to thank Franck Toussaint for the long-lasting collaboration in running ultralight trike airborne surveys.

Data Availability Statement

Data available upon request. Metadata and contact information for all datasets are provided on the Elvis geocatalogue: <https://elvis.ens-lyon.fr/geonetwork/srv/fr/catalog.search#/home>.

References

- Black, E., M. Blackburn, G. Harrison, B. Hoskins, and J. Methven. 2004. "Factors Contributing to the Summer 2003 European Heatwave." *Weather* 59: 217–223. <https://doi.org/10.1256/wea.74.04>.
- Bravard, J.-P., C. Amoros, G. Pautou, et al. 1997. "River Incision in South-East France: Morphological Phenomena and Ecological Effects." *Regulated Rivers: Research and Management* 13: 75–90. [https://doi.org/10.1002/\(SICI\)1099-1646\(199701\)13:1<75::AID-RRR444>3.0.CO;2-6](https://doi.org/10.1002/(SICI)1099-1646(199701)13:1<75::AID-RRR444>3.0.CO;2-6).
- Breton, V., J. Girel, and P. Janssen. 2023. "Long-Term Changes in the Riparian Vegetation of a Large, Highly Anthropized River: Towards Less Hygrophilous and More Competitive Communities." *Ecological Indicators* 155: 111015. <https://doi.org/10.1016/j.ecolind.2023.111015>.
- Brodribb, T. J., and N. M. Holbrook. 2003. "Stomatal Closure During Leaf Dehydration, Correlation With Other Leaf Physiological Traits." *Plant Physiology* 132: 2166–2173. <https://doi.org/10.1104/pp.103.023879>.
- Carbonneau, P. E., B. Belletti, M. Micotti, et al. 2020. "UAV-Based Training for Fully Fuzzy Classification of Sentinel-2 Fluvial Scenes." *Earth Surface Processes and Landforms* 45: 3120–3140. <https://doi.org/10.1002/esp.4955>.
- Ciężkowski, W., M. Kleniewska, and J. Chormański. 2020. "Thermal and Optical Indices for Wetland Habitats, Are They Showing the Same Thing?" *IEEE Journal of Selected Topics in Applied Earth Observations and Remote Sensing* 13: 3951–3957. <https://doi.org/10.1109/JSTARS.2020.3008864>.
- Comiti, F., M. Da Canal, N. Surian, L. Mao, L. Picco, and M. A. Lenzi. 2011. "Channel Adjustments and Vegetation Cover Dynamics in a Large Gravel bed River Over the Last 200 years." *Geomorphology* 125: 147–159. <https://doi.org/10.1016/j.geomorph.2010.09.011>.
- Décamps, H., M. Fortuné, F. Gazelle, and G. Pautou. 1988. "Historical Influence of Man on the Riparian Dynamics of a Fluvial Landscape." *Landscape Ecology* 1: 163–173. <https://doi.org/10.1007/BF00162742>.
- Dépret, T., N. Thommeret, H. Piégay, and E. Gautier. 2023. "Can Lateral Mobility Be Restored Along a Highly Domesticated Low-Energy Gravel-Bed River?" *Journal of Environmental Management* 325: 116485. <https://doi.org/10.1016/j.jenvman.2022.116485>.
- Dosskey, M. G., P. Vidon, N. P. Gurwick, C. J. Allan, T. P. Duval, and R. Lowrance. 2010. "The Role of Riparian Vegetation in Protecting and Improving Chemical Water Quality in Streams 1." *JAWRA Journal of the American Water Resources Association* 46: 261–277. <https://doi.org/10.1111/j.1752-1688.2010.00419.x>.
- Dufour, S. 2005. "Contrôles naturels anthropiques de la structure et de la dynamique des forêts riveraines." PhD thesis, Université Jean Moulin Lyon III, Lyon.
- Dufour, S., and H. Piégay. 2008. "Geomorphological Controls of *Fraxinus excelsior* Growth and Regeneration in Floodplain Forests." *Ecology* 89: 205–215. <https://doi.org/10.1890/06-1768.1>.
- Dugdale, S. J. 2016. "A Practitioner's Guide to Thermal Infrared Remote Sensing of Rivers and Streams: Recent Advances, Precautions and

- Considerations." *WIREs Water* 3: 251–268. <https://doi.org/10.1002/wat2.1135>.
- Dugdale, S. J., J. Franssen, E. Corey, N. E. Bergeron, M. Lapointe, and R. A. Cunjak. 2016. "Main Stem Movement of Atlantic Salmon Parr in Response to High River Temperature." *Ecology of Freshwater Fish* 25: 429–445. <https://doi.org/10.1111/eff.12224>.
- Dugdale, S. J., C. A. Kelleher, I. A. Malcolm, S. Caldwell, and D. M. Hannah. 2019. "Assessing the Potential of Drone-Based Thermal Infrared Imagery for Quantifying River Temperature Heterogeneity." *Hydrological Processes* 33: 1152–1163. <https://doi.org/10.1002/hyp.13395>.
- Dugdale, S. J., J. Klaus, and D. M. Hannah. 2022. "Looking to the Skies: Realising the Combined Potential of Drones and Thermal Infrared Imagery to Advance Hydrological Process Understanding in Headwaters." *Water Resources Research* 58: e2021WR031168. <https://doi.org/10.1029/2021WR031168>.
- Dugdale, S. J., I. A. Malcolm, K. Kantola, and D. M. Hannah. 2018. "Stream Temperature Under Contrasting Riparian Forest Cover: Understanding Thermal Dynamics and Heat Exchange Processes." *Science of the Total Environment* 610–611: 1375–1389. <https://doi.org/10.1016/j.scitotenv.2017.08.198>.
- Dumas, S. 2017. "Inventaire des boisements forestiers de la Basse Vallée de l'Ain." Office National des Forêts.
- Dumas, S., and V. Perrin. 2006. "Le suivi de la forêt alluviale de la Basse Vallée de l'Ain: Inventaire de niveau II de 2006." Office National des Forêts.
- Fairfax, E., and E. E. Small. 2018. "Using Remote Sensing to Assess the Impact of Beaver Damming on Riparian Evapotranspiration in an Arid Landscape." *Ecohydrology* 11: e1993. <https://doi.org/10.1002/eco.1993>.
- Gerle, F., P. Malherbe, C. Boisselet, et al. 2023. "Intrinsic Water Use Efficiency Estimate: An Isotopic Method."
- Godfroy, J., J. Lejot, L. Demarchi, S. Bizzi, K. Michel, and H. Piégay. 2023. "Combining Hyperspectral, LiDAR, and Forestry Data to Characterize Riparian Forests Along Age and Hydrological Gradients." *Remote Sensing* 15: 17. <https://doi.org/10.3390/rs15010017>.
- Gokool, S., C. Jarman, E. Riddell, A. Swemmer, R. Lerm, and K. T. Chetty. 2017. "Quantifying Riparian Total Evaporation Along the Groot Letaba River: A Comparison Between Infilled and Spatially Downscaled Satellite Derived Total Evaporation Estimates." *Journal of Arid Environments* 147: 114–124. <https://doi.org/10.1016/j.jaridenv.2017.07.014>.
- González del Tánago, M., V. Martínez-Fernández, F. C. Aguiar, et al. 2021. "Improving River Hydromorphological Assessment Through Better Integration of Riparian Vegetation: Scientific Evidence and Guidelines." *Journal of Environmental Management* 292: 112730. <https://doi.org/10.1016/j.jenvman.2021.112730>.
- Hsiao, T. C., and E. Acevedo. 1974. "Plant Responses to Water Deficits, Water-Use Efficiency, and Drought Resistance." *Agricultural Meteorology* 14: 59–84. [https://doi.org/10.1016/0002-1571\(74\)90011-9](https://doi.org/10.1016/0002-1571(74)90011-9).
- Janssen, P., J. C. Stella, H. Piégay, et al. 2020. "Divergence of Riparian Forest Composition and Functional Traits From Natural Succession Along a Degraded River With Multiple Stressor Legacies." *Science of the Total Environment* 721: 137730. <https://doi.org/10.1016/j.scitotenv.2020.137730>.
- Jones, H. G. 1999. "Use of Infrared Thermometry for Estimation of Stomatal Conductance as a Possible Aid to Irrigation Scheduling." *Agricultural and Forest Meteorology* 95: 139–149. [https://doi.org/10.1016/S0168-1923\(99\)00030-1](https://doi.org/10.1016/S0168-1923(99)00030-1).
- Jones, M. M., and H. M. Rawson. 1979. "Influence of Rate of Development of Leaf Water Deficits Upon Photosynthesis, Leaf Conductance, Water Use Efficiency, and Osmotic Potential in Sorghum." *Physiologia Plantarum* 45: 103–111. <https://doi.org/10.1111/j.1399-3054.1979.tb01672.x>.
- Kibler, C. L., E. C. Schmidt, D. A. Roberts, et al. 2021. "A Brown Wave of Riparian Woodland Mortality Following Groundwater Declines During the 2012–2019 California Drought." *Environmental Research Letters* 16: 084030. <https://doi.org/10.1088/1748-9326/ac1377>.
- Klein, T., E. Rotenberg, F. Tatarinov, and D. Yakir. 2016. "Association Between Sap Flow-Derived and Eddy Covariance-Derived Measurements of Forest Canopy CO₂ Uptake." *The New Phytologist* 209: 436–446. <https://doi.org/10.1111/nph.13597>.
- Lague, D., and B. Feldmann. 2020. "Topo-Bathymetric Airborne LiDAR for Fluvial-Geomorphology Analysis." In *Remote Sensing of Geomorphology, Developments in Earth Surface Processes*, edited by S. M. M. Paolo Tarolli, 25–54. Amsterdam, Netherlands: Elsevier. <https://doi.org/10.1016/B978-0-444-64177-9.00002-3>.
- Lambs, L., M. Loubiat, J. Girel, J. Tissier, J.-P. Peltier, and G. Marigo. 2006. "Survival and Acclimatation of *Populus nigra* to Drier Conditions After Damming of an Alpine River, Southeast France." *Annals of Forest Science* 63: 377–385. <https://doi.org/10.1051/forest:2006018>.
- Lejot, J., H. Piégay, P. D. Hunter, B. Moulin, and M. Gagnage. 2011. "Utilisation de la télédétection pour la caractérisation des corridors fluviaux: exemples d'applications et enjeux actuels." *Géomorphologie: Relief, Processus, Environnement* 17: 157–172. <https://doi.org/10.4000/geomorphologie.9362>.
- Liang, J., and J. Zhang. 1999. "The Relations of Stomatal Closure and Reopening to Xylem ABA Concentration and Leaf Water Potential During Soil Drying and Rewatering." *Plant Growth Regulation* 29: 77–86. <https://doi.org/10.1023/A:1006207900619>.
- Lurtz, M. R., R. R. Morrison, T. K. Gates, G. B. Senay, A. S. Bhaskar, and D. G. Ketchum. 2020. "Relationships Between Riparian Evapotranspiration and Groundwater Depth Along a Semiarid Irrigated River Valley." *Hydrological Processes* 34: 1714–1727. <https://doi.org/10.1002/hyp.13712>.
- Luterbacher, J., D. Dietrich, E. Xoplaki, M. Grosjean, and H. Wanner. 2004. "European Seasonal and Annual Temperature Variability, Trends, and Extremes Since 1500." *Science* 303: 1499–1503. <https://doi.org/10.1126/science.1093877>.
- Marteau, B., K. Michel, and H. Piégay. 2022. "Can Gravel Augmentation Restore Thermal Functions in Gravel-Bed Rivers? A Need to Assess Success Within a Trajectory-Based Before–After Control–Impact Framework." *Hydrological Processes* 36: e14480. <https://doi.org/10.1002/hyp.14480>.
- Marteau, B., H. Piégay, A. Chandresris, K. Michel, and L. Vaudor. 2022. "Riparian Shading Mitigates Warming but Cannot Revert Thermal Alteration by Impoundments in Lowland Rivers." *Earth Surface Processes and Landforms* 47: 2209–2229. <https://doi.org/10.1002/esp.5372>.
- Mayes, M., K. K. Caylor, M. B. Singer, J. C. Stella, D. Roberts, and P. Nagler. 2020. "Climate Sensitivity of Water Use by Riparian Woodlands at Landscape Scales." *Hydrological Processes* 34: 4884–4903. <https://doi.org/10.1002/hyp.13942>.
- Monclus, R., E. Dreyer, M. Villar, et al. 2006. "Impact of Drought on Productivity and Water Use Efficiency in 29 Genotypes of *Populus deltoides* × *Populus nigra*." *The New Phytologist* 169: 765–777. <https://doi.org/10.1111/j.1469-8137.2005.01630.x>.
- Naiman, R., H. Décamps, J. Pastor, and C. A. Johnston. 1988. "The Potential Importance of Boundaries of Fluvial Ecosystems." *Journal of the North American Benthological Society* 7: 289–306. <https://doi.org/10.2307/1467295>.
- Naiman, R. J., H. Decamps, and M. Pollock. 1993. "The Role of Riparian Corridors in Maintaining Regional Biodiversity." *Ecological Applications* 3: 209–212. <https://doi.org/10.2307/1941822>.
- Neale, C. M. U., H. Geli, S. Taghvaeian, et al. 2011. "Estimating Evapotranspiration of Riparian Vegetation Using High Resolution Multispectral, Thermal Infrared and Lidar Data." In *Remote Sensing for Agriculture, Ecosystems, and Hydrology XIII*, 254–262. Prague, Czech Republic: SPIE Remote Sensing. <https://doi.org/10.1117/12.903246>.

- O'Briain, R. 2019. "Climate Change and European Rivers: An Eco-Hydromorphological Perspective." *Ecohydrology* 12: e2099. <https://doi.org/10.1002/eco.2099>.
- Poff, N. L., J. D. Olden, D. M. Merritt, and D. M. Pepin. 2007. "Homogenization of Regional River Dynamics by Dams and Global Biodiversity Implications." *Proceedings of the National Academy of Sciences* 104: 5732–5737. <https://doi.org/10.1073/pnas.0609812104>.
- Redana, M., L. T. Lancaster, X. Y. Chong, Y. Y. Lip, and C. Gibbins. 2024. "An Open-Source Method for Producing Reliable Water Temperature Maps for Ecological Applications Using Non-radiometric Sensors." *Remote Sensing Applications: Society and Environment* 34: 101184. <https://doi.org/10.1016/j.rsase.2024.101184>.
- Riis, T., M. Kelly-Quinn, F. C. Aguiar, et al. 2020. "Global Overview of Ecosystem Services Provided by Riparian Vegetation." *Bioscience* 70: 501–514. <https://doi.org/10.1093/biosci/biaa041>.
- Rivaes, R., P. M. Rodríguez-González, A. Albuquerque, A. N. Pinheiro, G. Egger, and M. T. Ferreira. 2013. "Riparian Vegetation Responses to Altered Flow Regimes Driven by Climate Change in Mediterranean Rivers." *Ecohydrology* 6: 413–424. <https://doi.org/10.1002/eco.1287>.
- Rohde, M. M., J. C. Stella, D. A. Roberts, and M. B. Singer. 2021. "Groundwater Dependence of Riparian Woodlands and the Disrupting Effect of Anthropogenically Altered Streamflow." *Proceedings of the National Academy of Sciences* 118: e2026453118. <https://doi.org/10.1073/pnas.2026453118>.
- Rollet, A. J. 2007. "Etude et gestion de la dynamique sédimentaire d'un tronçon fluvial à l'aval d'un barrage: le cas de la basse vallée de l'Ain." PhD thesis, Université Jean Moulin Lyon 3.
- Rollet, A. J., H. Piégay, S. Dufour, G. Bornette, and H. Persat. 2014. "Assessment of Consequences of Sediment Deficit on a Gravel River Bed Downstream of Dams in Restoration Perspectives: Application of a Multicriteria, Hierarchical and Spatially Explicit Diagnosis." *River Research and Applications* 30: 939–953. <https://doi.org/10.1002/rra.2689>.
- Roux, C., A. Alber, M. Bertrand, L. Vaudor, and H. Piégay. 2015. "'FluvialCorridor': A New ArcGIS Toolbox Package for Multiscale Riverscape Exploration." *Geomorphology, Geomorphology in the Geocomputing Landscape: GIS, DEMs, Spatial Analysis and Statistics* 242: 29–37. <https://doi.org/10.1016/j.geomorph.2014.04.018>.
- Sankey, T., K. Hultine, D. Blasini, et al. 2021. "UAV Thermal Image Detects Genetic Trait Differences Among Populations and Genotypes of Fremont Cottonwood (*Populus fremontii*, Salicaceae)." *Remote Sensing in Ecology and Conservation* 7: 245–258. <https://doi.org/10.1002/rse2.185>.
- Scholander, P. F., E. D. Bradstreet, E. A. Hemmingsen, and H. T. Hammel. 1965. "Sap Pressure in Vascular Plants." *Science* 148: 339–346. <https://doi.org/10.1126/science.148.3668.339>.
- Scott, M. L., G. C. Lines, and G. T. Auble. 2000. "Channel Incision and Patterns of Cottonwood Stress and Mortality Along the Mojave River, California." *Journal of Arid Environments* 44: 399–414. <https://doi.org/10.1006/jare.1999.0614>.
- Seibt, U., A. Rajabi, H. Griffiths, and J. A. Berry. 2008. "Carbon Isotopes and Water Use Efficiency: Sense and Sensitivity." *Oecologia* 155: 441–454. <https://doi.org/10.1007/s00442-007-0932-7>.
- Simon, A., and A. J. C. Collison. 2002. "Quantifying the Mechanical and Hydrologic Effects of Riparian Vegetation on Streambank Stability." *Earth Surface Processes and Landforms* 27: 527–546. <https://doi.org/10.1002/esp.325>.
- Singer, M. B., J. C. Stella, S. Dufour, H. Piégay, R. J. S. Wilson, and L. Johnstone. 2013. "Contrasting Water-Uptake and Growth Responses to Drought in Co-occurring Riparian Tree Species." *Ecohydrology* 6: 402–412. <https://doi.org/10.1002/eco.1283>.
- Smith, S. D., A. B. Wellington, J. L. Nachlinger, and C. A. Fox. 1991. "Functional Responses of Riparian Vegetation to Streamflow Diversion in the Eastern Sierra Nevada." *Ecological Applications* 1: 89–97. <https://doi.org/10.2307/1941850>.
- Stella, J. C., J. Riddle, H. Piégay, M. Gagnage, and M.-L. Trémélo. 2013. "Climate and Local Geomorphic Interactions Drive Patterns of Riparian Forest Decline Along a Mediterranean Basin River." *Geomorphology, Process Geomorphology and Ecosystems: Disturbance Regimes and Interactions* 202: 101–114. <https://doi.org/10.1016/j.geomorph.2013.01.013>.
- Stella, J. C., P. M. Rodríguez-González, S. Dufour, and J. Bendix. 2013. "Riparian Vegetation Research in Mediterranean-Climate Regions: Common Patterns, Ecological Processes, and Considerations for Management." *Hydrobiologia* 719: 291–315. <https://doi.org/10.1007/s10750-012-1304-9>.
- Tabacchi, E., L. Lambs, H. Guilloy, A.-M. Planty-Tabacchi, E. Muller, and H. Décamps. 2000. "Impacts of Riparian Vegetation on Hydrological Processes." *Hydrological Processes* 14: 2959–2976. [https://doi.org/10.1002/1099-1085\(200011/12\)14:16/17<2959::AID-HYP129>3.0.CO;2-B](https://doi.org/10.1002/1099-1085(200011/12)14:16/17<2959::AID-HYP129>3.0.CO;2-B).
- Vernay, A., X. Tian, J. Chi, et al. 2020. "Estimating Canopy Gross Primary Production by Combining Phloem Stable Isotopes With Canopy and Mesophyll Conductances." *Plant, Cell & Environment* 43: 2124–2142. <https://doi.org/10.1111/pce.13835>.
- Viger, M., H. K. Smith, D. Cohen, et al. 2016. "Adaptive Mechanisms and Genomic Plasticity for Drought Tolerance Identified in European Black Poplar (*Populus nigra* L.)." *Tree Physiology* 36: 909–928. <https://doi.org/10.1093/treephys/tpw017>.
- Volaire, F. 2018. "A Unified Framework of Plant Adaptive Strategies to Drought: Crossing Scales and Disciplines." *Global Change Biology* 24: 2929–2938. <https://doi.org/10.1111/gcb.14062>.
- Wawrzyniak, V., P. Allemand, S. Bailly, J. Lejot, and H. Piégay. 2017. "Coupling LiDAR and Thermal Imagery to Model the Effects of Riparian Vegetation Shade and Groundwater Inputs on Summer River Temperature." *Science of the Total Environment* 592: 616–626. <https://doi.org/10.1016/j.scitotenv.2017.03.019>.
- Wawrzyniak, V., H. Piégay, P. Allemand, L. Vaudor, R. Goma, and P. Grandjean. 2016. "Effects of Geomorphology and Groundwater Level on the Spatio-Temporal Variability of Riverine Cold Water Patches Assessed Using Thermal Infrared (TIR) remote Sensing." *Remote Sensing of Environment* 175: 337–348. <https://doi.org/10.1016/j.rse.2015.12.050>.
- Whitledge, G. W., C. F. Rabeni, G. Annis, and S. P. Sowa. 2006. "Riparian Shading and Groundwater Enhance Growth Potential for Smallmouth Bass in Ozark Streams." *Ecological Applications* 16: 1461–1473. [https://doi.org/10.1890/1051-0761\(2006\)016\[1461:RSAGEG\]2.0.CO;2](https://doi.org/10.1890/1051-0761(2006)016[1461:RSAGEG]2.0.CO;2).
- Wilbur, N. M., A. M. O'Sullivan, K. T. B. MacQuarrie, T. Linnansaari, and R. A. Curry. 2020. "Characterizing Physical Habitat Preferences and Thermal Refuge Occupancy of Brook Trout (*Salvelinus fontinalis*) and Atlantic Salmon (*Salmo salar*) at High River Temperatures." *River Research and Applications* 36: 769–783. <https://doi.org/10.1002/rra.3570>.

Appendix A

TABLE A1 | Dates for which leaf and phloem sampling was conducted during 2022.

	Campaign date							
	May 5	May 25	June 10	June 28	July 19	August 9	August 23	September 27
Leaf	X	X	X	X	X	X	X	X
Phloem	X		X		X		X	X

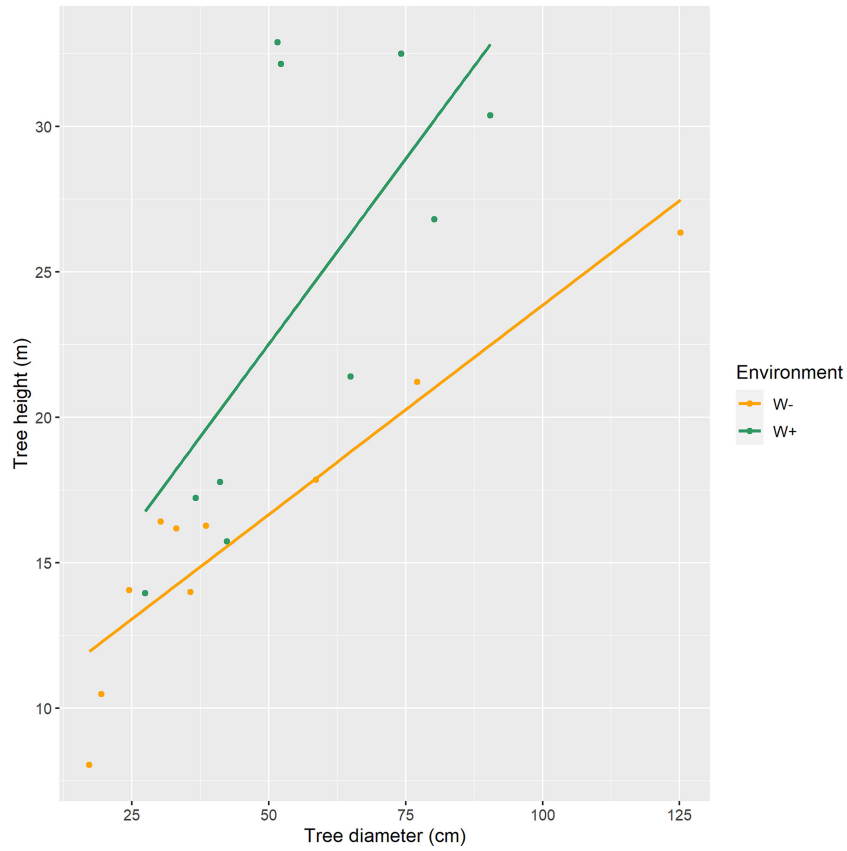


FIGURE A1 | Relationship between tree height and tree diameter on the W+ site ($r^2=0.47, p=0.0285$) and the W- site ($r^2=0.85, p=0.0001$).

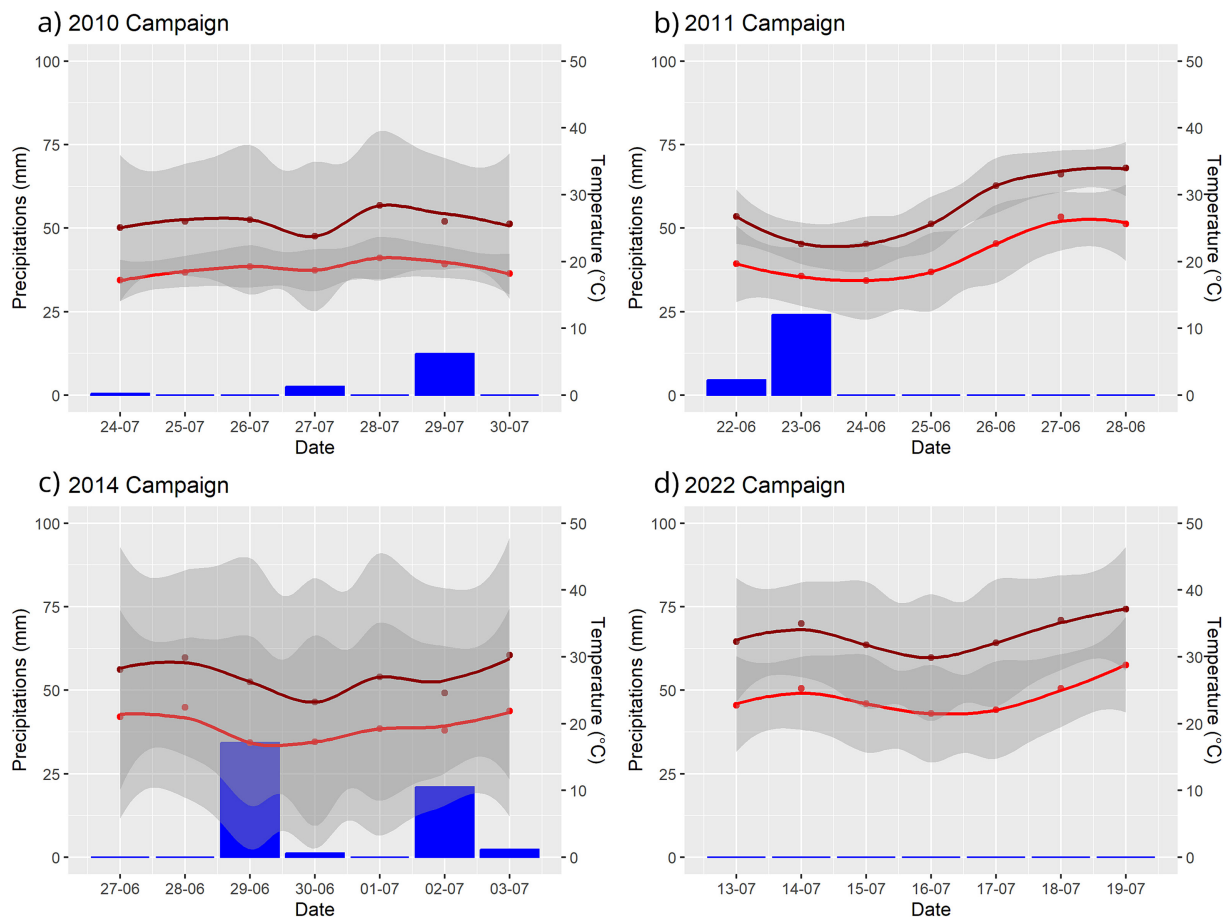


FIGURE A2 | Precipitation (blue), daily mean (red) and daily maximum (dark red) temperatures for a 7-day period preceding each airborne TIR campaign: (a) 2010, (b) 2011, (c) 2014 and (d) 2022.

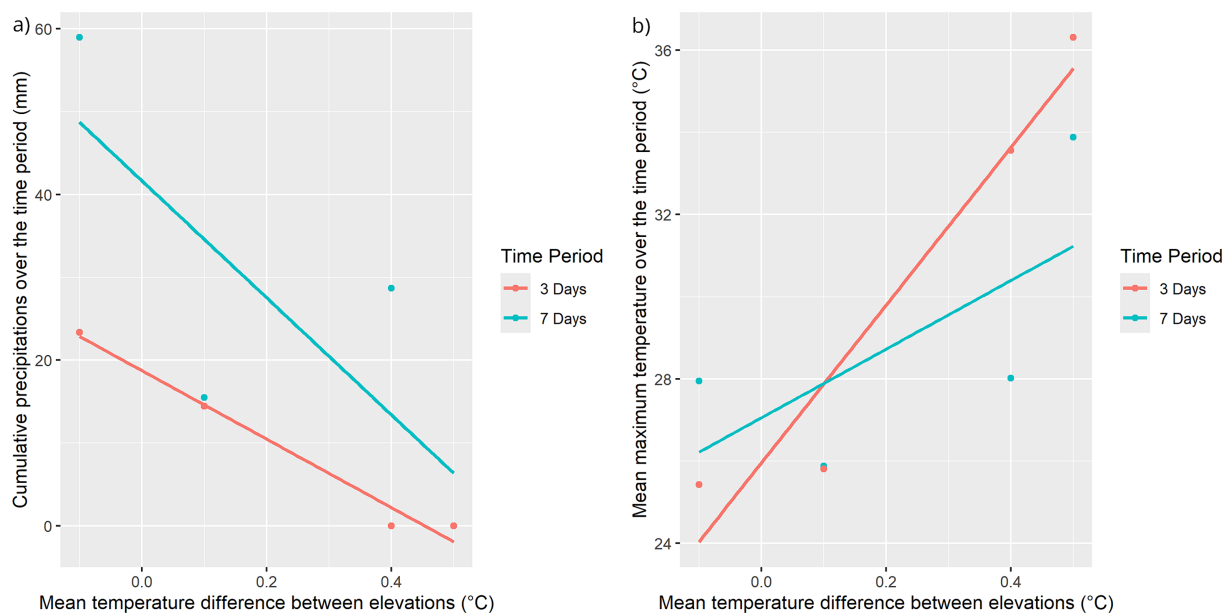


FIGURE A3 | Relationship between (a) cumulative precipitations and (b) mean maximum temperature for a 3-day or 7-day time period and the observed difference in mean temperatures from TIR data between the two elevation classes: connected (<2.5m from base flow) and disconnected (>2.5m from base flow).